HHS Public Access

Author manuscript

J Nucl Med. Author manuscript; available in PMC 2015 December 26.

Published in final edited form as:

J Nucl Med. 2014 July ; 55(7): 1106–1111. doi:10.2967/jnumed.113.130161.

Activity of P-glycoprotein, a β-amyloid Transporter at the Blood-Brain Barrier, is Compromised in Patients with Mild Alzheimer's Disease

Anand K. Deo[1], **Soo Borson**[2], **Jeanne M. Link**[3], **Karen Domino**[4], **Janet F. Eary**[3], **Ban Ke**[1], **Todd L. Richards**[3], **David A. Mankoff**[3], **Satoshi Minoshima**[3], **Finbarr O'Sullivan**[3,5], **Sara Eyal**[1], **Peng Hsiao**[1], **Ken Maravilla**[3], and **Jashvant D. Unadkat**[1,*]

[1]Department of Pharmaceutics, University of Washington, Seattle, P.O. Box 357610, WA 98195, USA [2]Department of Psychiatry and Behavioral Sciences, University of Washington, Seattle, WA 98195, USA [3]Department of Radiology, University of Washington, Seattle, WA 98195, USA [4]Department of Anesthesiology, University of Washington, Seattle, WA 98195, USA [5]Department of Statistics, University College Cork, Cork, Ireland

Abstract

Animal and histopathological studies of human brain support a role for P-glycoprotein (P-gp) in clearance of cerebral β-amyloid (Aβ) across the blood brain barrier (BBB). We tested the hypothesis that BBB P-gp activity is diminished in Alzheimer's disease (AD) by accounting for AD-related reduction in regional cerebral blood flow (rCBF).

Methods—We compared P-gp activity in mild AD patients (n=9) and cognitively normal, age-matched controls (n=9) using positron emission tomography (PET) with a labeled P-gp substrate, [^{11}C]-verapamil, and [^{15}O]-water to measure rCBF. BBB P-gp activity was expressed as the [^{11}C]-verapamil radioactivity extraction ratio (ER={[^{11}C]-verapamil brain distributional clearance, K_1}/rCBF).

Results—Compared to controls, BBB P-gp activity was significantly lower in the parietotemporal, frontal, posterior cingulate cortices and hippocampus of mild AD subjects.

Conclusion—BBB P-gp activity in brain regions affected by AD is reduced and is independent of rCBF. This study improves on prior work by eliminating the confounding effect that reduced rCBF has on assessment of BBB P-gp activity and suggests that impaired P-gp activity may contribute to cerebral Aβ accumulation in AD. P-gp induction/activation to increase cerebral Aβ clearance could constitute a novel preventive or therapeutic strategy for AD.

Address correspondence to: Jashvant D. Unadkat, Department of Pharmaceutics, University of Washington, Box 357610, Seattle, Washington 98195, USA. Fax: (206) 543 3204; Phone: (206) 685 2869; jash@u.washington.edu.

DISCLOSURE

The authors declare no conflict of interest. The study was supported by grants to JDU from AHAF (A2007-086) and the National Institute of Aging (031485), and to PH from NCRR Grant TL1 RR 025016, the ITHS TL1 Multidisciplinary Predoctoral Clinical Research Training Program (PHS2271).

Keywords

Alzheimer's disease; blood-brain barrier; P-glycoprotein activity; PET imaging; relative extraction ratio

The neuropathological hallmarks of Alzheimer's disease (AD) are regional deposition of amyloid plaques, neurofibrillary tangles consisting of hyperphosphorylated tau protein, inflammation, and neurodegeneration, particularly in parietal and temporal cortex, hippocampus and amygdala (1). Clinically useful disease-modifying treatments for AD have been elusive. Approved drug therapies, while providing some symptomatic benefits, do not alter the fundamental course or outcome of the disease, adding impetus for research on new mechanisms of disease pathogenesis that might lead to novel therapeutic approaches. Substantial current investment in development of therapeutic strategies aimed at modifying Aβ accumulation (2) have been justified by evidence that deficient Aβ clearance, a process known to be impaired in AD (3–6), is associated with toxic neuronal (7) and vascular (8–10) effects and irreversible neurodegeneration.

Studies in mouse models of AD have demonstrated that endogenous P-gp plays a decisive role in Aβ clearance from the CNS. As compared to wild-type mice, *in vivo* cerebral clearance of labeled Aβ40 and Aβ42 is decreased by 50% in P-gp knock-out mice (3). In addition, the brain interstitial concentration of Aβ in hAPP transgenic mice (an animal model for AD) is increased by a selective P-gp inhibitor (3) but decreased by a P-gp inducer (4). Furthermore, the progeny of hAPP/P-gp knockout mice accumulate Aβ in the brain more extensively than hAPP/P-gp wild type mice (3). In hippocampal tissue from AD brain, Aβ deposition is higher and P-gp expression lower than in age-matched control tissue (11). Based on these compelling data, we hypothesized that P-gp activity at the BBB is compromised in mild AD patients. Recently, van Assema et al., addressed this question using (*R*)-[^{11}C]-verapamil and PET imaging to measure P-gp activity at the BBB in mild to moderately demented AD patients (12). Our work improves upon this prior report by simultaneously measuring regional cerebral blood flow (rCBF) using [^{15}O] water in addition to [^{11}C]-verapamil to measure regional P-gp function. Since rCBF is reduced in areas affected by AD, its measurement is necessary to evaluate [^{11}C]-verapamil kinetics as a measure of regional P-gp function at the BBB (13). Here we report results of a positron emission tomography (PET) imaging study to test this hypothesis in mild AD patients using a combination of [^{15}O] water and [^{11}C]-verapamil to measure P-gp activity at the human BBB, an approach we have successfully used previously in other settings (13, 14).

MATERIALS AND METHODS

Subjects

Eighteen older adults (9 normal, 9 mild AD) were studied after obtaining signed informed consent (from legal next of kin for AD) using procedures approved by the University of Washington Institutional Review Board and the Radiation Safety and Radioactive Drug Research committees. Subjects were classified according to the Alzheimer's Disease Research Centers Uniform Data Set after excluding any with major medical co-morbidity

and those taking systemic drugs or herbal products that induce, inhibit, or act as substrates for P-gp and ruling out surgical brain lesions and stroke by non-contrast brain MRI. AD subjects were on a stable therapeutic dose of cognitive enhancing medications (a cholinesterase inhibitor and/or memantine) for at least 12 weeks at the time of study. Sample size calculations, based on our study in healthy volunteers (age 20–50) (17), assumed ≥50% difference in BBB P-gp activity between AD and control subjects, because a smaller effect would not be clinically or scientifically significant. Seven subjects per group were sufficient to provide 80% power to detect this difference at alpha = 0.05.

PET Imaging

Radiosynthesis was conducted using methods we have described previously (17). Briefly, [^{11}C]-verapamil was produced by bubbling [^{11}C]-CH_3I into 1–2 mg of (±) norverapamil in 0.35 mL of anhydrous acetonitrile and heating at 100°C for 5 minutes. The product was purified by separation on an Inertsil ODS2 (6X150 mm, 5 μM) column at 46°C in 35 % ethanol 65% phosphate buffered saline by volume. The specific activity of [^{11}C]-verapamil was determined using UV absorption at 263 nm or mass spectrometry (ES+) to measure μmoles per mL of drug product and dividing radioactivity (mCi) per mL by μmoles per mL. The specific activity [^{11}C]-verapamil was 40,700 ± 18,500 GBq/mmol (range 20,720 to 111,000 GBq/mmol) at injection. The variability in specific activity was primarily due to to time between end of bombardment and injection. The imaging protocol was similar to that we have described previously (17) except, to reduce study burden for older subjects, venous blood sampling replaced arterial sampling for 12 (9 AD and 3 controls) subjects.

Each subject first received an IV bolus of [^{15}O]-water (5.18±0.74 MBq/kg), to measure rCBF). Brain images were acquired using a GE Advance PET Scanner in 3D mode with the following sequence of time bins: 16 × 2 seconds, 8 × 4 seconds, 8 × 8 seconds, 10 × 16 seconds respectively. When obtained, arterial samples (1 ml each, every 15 seconds for first 2 minutes, every 30 seconds for next 1.5 minutes and at 4 and 5 minutes) were drawn manually using a Hi-Flo™ 5 Gang, 3-way manifold. Venous samples from the contralateral arm (1 ml) were obtained every minute for 5 min. All blood samples were drawn in pre-weighed tubes and counted.

P-gp activity at the BBB was determined as a function of distributional clearance (K_1) of [^{11}C]-verapamil radioactivity across the BBB (16, 17). Approximately 15 minutes after [^{15}O]-water administration, [^{11}C]-verapamil (5.18±1.11 MBq/kg, 0.06±0.03 μg/kg) was administered intravenously as a 1 minute infusion. Images were acquired using the following post-injection sequence of time bins: 16 × 5 seconds, 7 × 10 seconds, 5 × 30 seconds, 5 × 60 seconds and 5 × 120 seconds. Arterial samples (1 ml each when obtained; every 15 seconds for first minute, every 20 seconds for next 1 minute, every 30 seconds for next 1 minute, every 1 minute for next 5 minutes, every 2 minutes for next 4 minutes, and finally at 15 and 20 minutes) and venous samples (1 ml at 1, 2, 5, 10, 15 and 20 minutes) were obtained manually. Aliquots of 200 μl of blood and 200 μl of plasma were counted for radioactivity as described previously (17).

Data Analysis

Final measurements of rCBF and P-gp activity in each subject were expressed relative to the subject's own cerebellum CBF and [^{11}C]-verapamil K_1 values. The cerebellum was used as a reference region because its CBF is unaffected by AD, the structure is large and therefore provides a reliable signal for image analysis (19–21) and it serves to account for dose variability and any bias in estimating verapamil K_1 and CBF by arterial image analysis. This approach obviated the need to obtain absolute arterial blood concentrations of [^{15}O]-water or [^{11}C]-verapamil for use as input function for kinetic modeling of the data. Nevertheless, for modeling purposes, it was useful to have arterial input functions in an approximately correct Y-scale range. To do so, we estimated the arterial [^{15}O]-water and [^{11}C]-verapamil concentrations by extraction from the dynamic PET images (22) and scaled them using late venous measurements and the average arterial to venous (A-V) ratio at pseudo-equilibrium, obtained from control subjects who had both arterial and venous sampling (n=6). An automated algorithm was used to extract the arterial time course of the tracer from image data (22). This method uses a segmentation procedure to focus on a suitable blood pool region within the field of view. Data within this region were analyzed by a Bayesian penalty optimization that accounted for spillover of activity from surrounding tissue and imperfect recovery due to limitations in scanner spatial resolution (~4mm). The construction of the Bayesian prior distribution for arterial blood curves followed our previous approach (22) based on earlier studies that directly measured arterial blood curves by arterial catheterization (15).

PET image reconstruction and data analysis were conducted as described previously (13). Image and blood data were corrected for radioactive decay. MRI images were co-registered to the PET images using PMOD 3.0 (PMOD Technologies, Zurich, Switzerland). Parametric maps for rCBF and verapamil K_1 were derived from the respective dynamic PET images and estimated arterial concentrations (0–2 min for [^{15}O]-water or 0–10 min for [^{11}C]-verapamil when metabolism of verapamil in young healthy volunteers is minimal; verapamil metabolism is further decreased in elderly subjects (23). Parametric maps were generated by fitting a one tissue compartment (Zhou GRRSC) model in PXMOD (PMOD *ver* 3.0) to the data as described previously (16).

Individual rCBF and verapamil K_1 parametric maps were co-registered with density corrected (attenuated) PET brain images for each subject, and each set of individual parametric map was coregistered to the Montreal Neurological Institute (MNI) standard brain using the MRI T1-weighted images and the PET brain transmission images as input into FSL's FLIRT software (http://www.fmrib.ox.ac.uk/fsl/flirt/index.html). rCBF and verapamil K_1 parametric images were normalized to the cerebellum signal to generate rCBFc and K_{1c} parametric maps, using an atlas-guided contour drawn to avoid regions near large blood vessels. Each pixel value of the PET images was divided by the average signal within the cerebellum-contoured region to create two different normalized maps. We further normalized K_{1c} to the rCBFc (ratio of regional [^{11}C]-verapamil K_{1c} and rCBFc) and generated relative regional ERc-grouped statistical parametric maps. The software Randomise (http://www.fmrib.ox.ac.uk/fsl/randomise/index.html) was used to perform a non-parametric voxel by voxel unpaired two-tailed t-test with multiple comparison

correction using the Threshold-Free Cluster Enhancement option (24) to compare PET parametric maps of AD subjects and controls. Automated anatomical labeling of differences in rCBFc or ERc was done by coregistering the maps to the standard MNI brain (25).

ROI Analysis

To quantify the magnitude of difference in rCBFc and ERc from the parametric approach, regions of interest (ROI) were contoured on left and right parietotemporal cortices, and cerebellum. The ROI were drawn using the software FSLVIEW and the anatomical location was validated based on the AAL atlas provided by MRIcro anatomical template http://www.cabiatl.com/mricro/mricro/template.html. Cerebellum normalized ^{11}C-verapamil K_1 (K_1c) and CBF (CBFc) values were obtained and verapamil relative extraction ratio (ERc) values were calculated for each region by normalizing K_1c with CBFc as per the equation below

$$\mathrm{ERc}=\mathrm{Ver}\,K_1c/\mathrm{CBFc}.$$

Semi-parametric Approach

A semi-independent confirmation of results was conducted using a semi-parametric approach. Tissue time-activity curves were obtained for ^{15}O-water and ^{11}C-verapamil in the ROIs for cerebellum, and left and right temporal and parietal cortices. rCBF was estimated by fitting a one compartment flow dispersion model using estimated [^{15}O]-water arterial concentrations and the tissue time-activity [^{15}O]-water concentrations in the cerebellum or the parieto-temporal cortices. Then, the cerebellum- normalized area under the curve of [^{11}C]-verapamil concentration-time profile (AUCc; 0–10 min) was estimated for these regions. These values were normalized to the cerebellum-normalized rCBF (rCBFc; 0–2 min) as per the equation below.

$$\frac{^{11}\mathrm{C\text{-}\ Verapamil\,AUC/Cerebellum\,AUC}}{\mathrm{rCBF/Cerebellum\,CBF}}=\frac{^{11}\mathrm{C\text{-}\ Ver\,AUCc}}{\mathrm{rCBFc}}$$

Statistics

Statistical comparisons for rCBFc and ERc data for ROI analysis (Fig. 2) and the semi-parametric approach (Fig. 3) were carried out using unpaired two-tailed *t*-tests (GraphPad 3.0).

RESULTS

Subjects

The subject sample (Table 1) showed no group differences for age (p=0.75), weight (p=0.34) or education (p=0.18). Cognitive (Mini-Cog^{TM} and Mini-Mental State Examination, MMSE) score differences between the groups (both p<0.0001) are typical of healthy vs. mildly demented AD subjects.

Cerebral Blood Flow In AD vs. Controls

Cerebellum-normalized statistical rCBF (rCBFc) maps demonstrated significant regional hypoperfusion ($p<0.05$) in posterior cingulate, left and right parietotemporal cortices, hippocampus, and frontal brain regions in AD vs. control subjects (Fig. 1A). rCBFc was also reduced in the posterior cingulate cortex and hippocampus, regions typically affected in early AD (Fig. 1A). Pons normalization, another brain region unaffected by AD yielded similar results (data not shown).

BBB P-gp activity in AD vs. Controls

Parametric Approach—Cerebellum-normalized relative regional extraction ratio (ERc) ([^{11}C]-verapamil K_{1c} /rCBFc) represents regional BBB P-gp activity (13). Since P-gp reduces net blood-to-brain clearance of verapamil (K_1 or ER) across the BBB, ER is inversely related to P-gp activity. Lower P-gp activity, implying reduced ability to export Aβ, translates into higher ER (13). Comparison of ERc-grouped statistical parametric maps in the sagittal plane demonstrated a significant ($p<0.05$) bilateral increase in verapamil ERc (i.e. our hypothesized reduction in P-gp activity) in parietotemporal and frontal lobes in AD (Fig. 1B) compared to controls. P-gp activity was also decreased in the hippocampus and posterior cingulate cortex (Fig. 1B), regions where the earliest changes in AD are observed. The decrease in P-gp activity in AD was symmetrical in sagittal views of the parietotemporal cortices (Fig. 1B) but less so in frontal lobes (reduction more prominent on the left) and in coronal views of the parietotemporal cortex and hippocampus (more prominent on the right) (Fig. 1B). Not all brain regions showing reduced P-gp activity had reduced rCBFc; this discordance indicates that reduced P-gp activity cannot be attributed to regional hypoperfusion. Pons normalization yielded similar results (data not shown).

To quantify the magnitude of difference in cerebral blood flow and P-gp activity between AD and control subjects, ROI analysis was conducted on the parametric maps for the left and right parietotemporal cortices (Fig. 2). For these regions, cerebellum-normalized K_1 (K_1c) and CBF (CBFc) values were obtained and relative extraction ratio (ERc) values were calculated by the ratio K_1c/CBFc. Despite the variability, as expected, the rCBFc (Fig. 2A) and P-gp activity (ERc values) (Fig. 2B) were reduced in these brain regions of AD patients vs. controls, particularly in the temporal cortex and left parietal cortex ($p<0.05$). These ER values are numerically greater than unity because they are relative and not absolute values.

Semi-parametric Approach—Area under the tissue-activity time curve was computed to examine cerebral verapamil distribution, a method previously shown to approximate P-gp activity at the human BBB (13, 17). Despite the variability, this analysis also demonstrated decreased rCBFc in the left and right temporal cortices of the AD brain (Fig. 3A) but was less sensitive to the parietal cortical differences observed using the parametric approach, above. Similarly, [^{11}C]-verapamil AUCc normalized to rCBFc was significantly increased (representing reduced P-gp activity) in the left and right temporal and the left (but not the right) parietal cortices in AD (Fig. 3B).

DISCUSSION

P-gp activity was reduced by nearly 50% in parietotemporal and posterior cingulate cortex (Fig. 1), regions that constitute an AD 'signature' in PET studies measuring either rCBF (26–29) or metabolic activity (30, 31). P-gp activity in hippocampus and left frontal cortex was also reduced, consistent with known pathologic changes and metabolic imaging studies in AD (32–34). These findings support investigation of deficient P-gp activity as a possible pathogenic mechanism in AD, and call for studies of individuals in the pre-symptomatic phases of the disease. If P-gp activity is reduced during the early phases of amyloid accumulation, before neurodegenerative changes have become extensive and irreversible, therapies targeting enhancement of endogenous P-gp activity could become a new focus for drug development.

Measurement of rCBF is important for accurate estimation of regional P-gp activity at the BBB when using distribution clearance of [^{11}C]-verapamil into the brain as an index of BBB P-gp activity. Lipophilic P-gp PET ligands, including verapamil, are highly extracted by brain tissue when P-gp activity is absent or diminished, and therefore its distribution clearance (K_1) into the brain is sensitive to changes in rCBF (17, 35). Accurate estimation of P-gp activity at the BBB in AD, where rCBF is not constant across brain regions, depends on measuring the ER of verapamil (13). If K_1 is used instead, P-gp activity could appear constant even when reduced, since in the absence of changes in rCBF, reduced P-gp activity should result in higher K_1. But, in AD, this change in K_1 will be nullified or limited by disease-related regionally reduced blood flow. When ER is used as a measure of P-gp activity, reduced blood flow is accounted for and regions having reduced activity will be correctly reported by a higher ER. That is, the use of ER as the measure of P-gp activity at the BBB effectively addresses the confounding effect of regional differences in perfusion seen in AD. Further, normalizing K_{1c} to rCBFc and generating cerebellum-normalized relative regional extraction ratio (ERc)-grouped statistical parametric maps, made comparisons of AD and control ERs more stringent. We confirmed the above parametric analysis with a semi-parametric approach and verified that kinetic modeling of verapamil did not introduce bias.

A non-specific regional increase in BBB permeability to ^{11}C-verapamil is not likely to explain our observation of increased regional [^{11}C]-verapamil ERc in AD patients as overall BBB permeability is not strongly affected by AD (36). We observed an apparent dissociation between reduced P-gp activity and regional hypoperfusion in wide areas of brain in AD. This is a novel finding and suggests that, at the least, P-gp activity and rCBF report different aspects of the disease. If compromised P-gp activity proves to be part of the early pathogenetic cascade of AD, it could become a target for future novel therapeutics. van Assema et al., published a study testing the same hypothesis as proposed here, but using (*R*)-[^{11}C]-verapamil in mild to moderate AD patients (12). They concluded that P-gp function at the BBB function was reduced in AD based on the finding that the binding potential ($=k_3/k_4$) of (*R*)-[^{11}C]-verapamil in the brain of mild to moderate AD subjects was greater than that in age-matched healthy controls using a two-compartment model (12). Unlike our analysis using a one compartment model and a short scan time (over 10 min., when >80% of the radioactivity in the plasma is un-metabolized verapamil (16)), they used an extended

imaging time (60 min.), during which an increasing fraction of blood radioactivity (up to 50%) represents labeled metabolites (18), a problem which can confound interpretation of imaging data (16). In addition, we have previously shown that k_3 and k_4 are poorly estimated and likely to be confounded by binding of verapamil or metabolites to yet-unidentified brain constituents which might differ between AD and controls (e.g. amyloid plaques). Our approach improves on the analysis by van Assema et al. (12) by accounting for the perfusion-dependence of verapamil distribution and correcting for the confounding effect of regional differences in perfusion seen in AD. As expected, and consistent with our data, they found no difference in K_1, the distributional clearance of [^{11}C]-verapamil across the BBB in AD. Though we agree with van Assema et al. that P-gp activity is compromised in regions affected by AD (e.g. parietal and temporal cortex), there are important differences between their findings and ours. They found decreased P-gp activity in regions not typically affected in mild to moderate AD (e.g. occipital cortex) (31, 34), and also failed to observe diminished activity in brain regions uniformly involved early in the disease process (e.g. medial temporal lobe/hippocampus).

CONCLUSION

Our data are the first to demonstrate decreased P-gp activity at the BBB in brain regions typically affected in mild AD, using analytical methods not confounded by disease-related differences in rCBF. We cannot determine whether decreased P-gp activity plays a primary pathogenic role in reducing cerebral clearance of Aβ, or whether accumulation of Aβ, or other pathological events in AD, result in reduced BBB P-gp activity (37). Irrespective of any causal relationship, the end result is expected to be reduced cerebral clearance of Aβ. Increasing cerebral clearance of Aβ by inducing or activating BBB P-gp activity could constitute a novel therapeutic target to restore CNS Aβ homeostasis in patients with AD. Potent inducers of P-gp such as rifampin and dexamethasone are FDA-approved prescription drugs, and others are available over the counter (e.g. St. John’s wort). While these drugs can induce intestinal P-gp activity (38, 39), it is not clear whether their systemic concentrations would be sufficient to induce P-gp at the BBB. Studies to address this question are ongoing in our laboratory. If P-gp is found to be inducible at the BBB in AD, the next critical questions will be whether such treatment can arrest the progression of the disease, and at what point in disease evolution it should be initiated (40).

Acknowledgments

We thank Michelle Wanner, Pam Phan, Jeff Stevenson, Steve Shoner, Xuehi Li (Dept. of Radiology, Univ. of WA), Li Liu, Brian Kirby (Dept. of Pharmaceutics, Univ. of WA), and Mary Lessig (Dept. of Psychiatry and Behavioral Sciences) for their technical assistance.

References

1. Querfurth HW, LaFerla FM. Alzheimer's disease. New Eng J Med. 2010; 362:329–344. [PubMed: 20107219]
2. Ozudogru SN, Lippa CF. Disease modifying drugs targeting beta-amyloid. Am J Alzheimers Dis Other Demen. 2012; 27:296–300. [PubMed: 22815077]

3. Cirrito JR, Deane R, Fagan AM, et al. P-glycoprotein deficiency at the blood-brain barrier increases amyloid-beta deposition in an Alzheimer disease mouse model. J Clin Invest. 2005; 115:3285–3290. [PubMed: 16239972]
4. Hartz AM, Miller DS, Bauer B. Restoring blood-brain barrier P-glycoprotein reduces brain amyloid-beta in a mouse model of Alzheimer's disease. Mol Pharmacol. 2010; 77:715–723. [PubMed: 20101004]
5. Mawuenyega KG, Sigurdson W, Ovod V, et al. Decreased clearance of CNS beta-amyloid in Alzheimer's disease. Science. 2010; 330:1774. [PubMed: 21148344]
6. Vogelgesang S, Cascorbi I, Schroeder E, et al. Deposition of Alzheimer's beta-amyloid is inversely correlated with P-glycoprotein expression in the brains of elderly non-demented humans. Pharmacogenetics. 2002; 12:535–541. [PubMed: 12360104]
7. Hardy J, Selkoe DJ. The amyloid hypothesis of Alzheimer's disease: progress and problems on the road to therapeutics. Science. 2002; 297:353–356. [PubMed: 12130773]
8. Bailey TL, Rivara CB, Rocher AB, Hof PR. The nature and effects of cortical microvascular pathology in aging and Alzheimer's disease. Neurol Res. 2004; 26:573–578. [PubMed: 15265277]
9. de la Torre JC. Alzheimer's disease is a vasocognopathy: a new term to describe its nature. Neurol Res. 2004; 26:517–524. [PubMed: 15265269]
10. Zlokovic BV. Neurovascular mechanisms of Alzheimer's neurodegeneration. Trends Neurosci. 2005; 28:202–208. [PubMed: 15808355]
11. Wijesuriya HC, Bullock JY, Faull RL, Hladky SB, Barrand MA. ABC efflux transporters in brain vasculature of Alzheimer's subjects. Brain Res. 2010; 1358:228–238. [PubMed: 20727860]
12. van Assema DM, Lubberink M, Bauer M, et al. Blood-brain barrier P-glycoprotein function in Alzheimer's disease. Brain. 2012; 135:181–189. [PubMed: 22120145]
13. Eyal S, Ke B, Muzi M, et al. Regional P-glycoprotein activity and inhibition at the human blood-brain barrier as imaged by positron emission tomography. Clin Pharmacol Ther. 2010; 87:579–585. [PubMed: 20336065]
14. Ke AB, Eyal S, Chung FS, et al. Modeling cyclosporine A inhibition of the distribution of a P-glycoprotein PET ligand, 11C-verapamil, into the maternal brain and fetal liver of the pregnant nonhuman primate: impact of tissue blood flow and site of inhibition. J Nucl Med. 2013; 54:437–446. [PubMed: 23359659]
15. Chung FS, Eyal S, Muzi M, et al. Positron emission tomography imaging of tissue P-glycoprotein activity during pregnancy in the non-human primate. Br J Pharmacol. 2010; 159:394–404. [PubMed: 20002098]
16. Muzi M, Mankoff DA, Link JM, et al. Imaging of cyclosporine inhibition of P-glycoprotein activity using 11C-verapamil in the brain: studies of healthy humans. J Nucl Med. 2009; 50:1267–1275. [PubMed: 19617341]
17. Sasongko L, Link JM, Muzi M, et al. Imaging P-glycoprotein transport activity at the human blood-brain barrier with positron emission tomography. Clin Pharmacol Ther. 2005; 77:503–514. [PubMed: 15961982]
18. Lubberink M, Luurtsema G, van Berckel BN, et al. Evaluation of tracer kinetic models for quantification of P-glycoprotein function using (R)-[11C]verapamil and PET. J Cereb Blood Flow Metab. 2007; 27:424–433. [PubMed: 16757979]
19. Heiss WD, Szelies B, Kessler J, Herholz K. Abnormalities of energy metabolism in Alzheimer's disease studied with PET. Ann N Y Acad Sci. 1991; 640:65–71. [PubMed: 1776760]
20. McGeer PL, Kamo H, Harrop R, et al. Positron emission tomography in patients with clinically diagnosed Alzheimer's disease. CMAJ. 1986; 134:597–607. [PubMed: 3512063]
21. Minoshima S, Frey KA, Foster NL, Kuhl DE. Preserved pontine glucose metabolism in Alzheimer disease: a reference region for functional brain image (PET) analysis. J Comput Assist Tomogr. 1995; 19:541–547. [PubMed: 7622680]
22. O'Sullivan F, Kirrane J, Muzi M, et al. Kinetic quantitation of cerebral PET-FDG studies without concurrent blood sampling: statistical recovery of the arterial input function. IEEE Trans Med Imaging. 2010; 29:610–624. [PubMed: 19709971]

23. Schwartz JB, Capili H, Wainer IW. Verapamil stereoisomers during racemic verapamil administration: effects of aging and comparisons to administration of individual stereoisomers. Clin Pharmacol Ther. 1994; 56:368–376. [PubMed: 7955798]
24. Nichols TE, Holmes AP. Nonparametric permutation tests for functional neuroimaging: a primer with examples. Hum Brain Mapp. 2002; 15:1–25. [PubMed: 11747097]
25. Tzourio-Mazoyer N, Landeau B, Papathanassiou D, et al. Automated anatomical labeling of activations in SPM using a macroscopic anatomical parcellation of the MNI MRI single-subject brain. Neuroimage. 2002; 15:273–289. [PubMed: 11771995]
26. Bartenstein P, Minoshima S, Hirsch C, et al. Quantitative assessment of cerebral blood flow in patients with Alzheimer's disease by SPECT. Journal of nuclear medicine : official publication, Society of Nuclear Medicine. 1997; 38:1095–1101.
27. Duran FL, Zampieri FG, Bottino CC, Buchpiguel CA, Busatto GF. Voxel-based investigations of regional cerebral blood flow abnormalities in Alzheimer's disease using a single-detector SPECT system. Clinics. 2007; 62:377–384. [PubMed: 17823698]
28. Ishii K, Kitagaki H, Kono M, Mori E. Decreased medial temporal oxygen metabolism in Alzheimer's disease shown by PET. J Nucl Med. 1996; 37:1159–1165. [PubMed: 8965188]
29. Ishii K, Sasaki M, Yamaji S, Sakamoto S, Kitagaki H, Mori E. Demonstration of decreased posterior cingulate perfusion in mild Alzheimer's disease by means of H215O positron emission tomography. Eur J Nucl Med. 1997; 24:670–673. [PubMed: 9169576]
30. Minoshima S, Giordani B, Berent S, Frey KA, Foster NL, Kuhl DE. Metabolic reduction in the posterior cingulate cortex in very early Alzheimer's disease. Ann Neurol. 1997; 42:85–94. [PubMed: 9225689]
31. Mosconi L. Brain glucose metabolism in the early and specific diagnosis of Alzheimer's disease. FDG-PET studies in MCI and AD. Eur J Nucl Med Mol Imaging. 2005; 32:486–510. [PubMed: 15747152]
32. Cutler NR, Haxby JV, Duara R, et al. Clinical history, brain metabolism, and neuropsychological function in Alzheimer's disease. Ann Neurol. 1985; 18:298–309. [PubMed: 3876805]
33. Kumar A, Schapiro MB, Haxby JV, Grady CL, Friedland RP. Cerebral metabolic and cognitive studies in dementia with frontal lobe behavioral features. J Psychiatr Res. 1990; 24:97–109. [PubMed: 2213642]
34. Minoshima S, Frey KA, Koeppe RA, Foster NL, Kuhl DE. A diagnostic approach in Alzheimer's disease using three-dimensional stereotactic surface projections of fluorine-18-FDG PET. JNucl Med. 1995; 36:1238–1248. [PubMed: 7790950]
35. Lazarova N, Zoghbi SS, Hong J, et al. Synthesis and evaluation of [N-methyl-11C]N-desmethyl-loperamide as a new and improved PET radiotracer for imaging P-gp function. J Med Chem. 2008; 51:6034–6043. [PubMed: 18783208]
36. Starr JM, Farrall AJ, Armitage P, McGurn B, Wardlaw J. Blood-brain barrier permeability in Alzheimer's disease: a case-control MRI study. Psychiatry Res. 2009; 171:232–241. [PubMed: 19211227]
37. Kania KD, Wijesuriya HC, Hladky SB, Barrand MA. Beta amyloid effects on expression of multidrug efflux transporters in brain endothelial cells. Brain Res. 2011; 1418:1–11. [PubMed: 21920506]
38. Greiner B, Eichelbaum M, Fritz P, et al. The role of intestinal P-glycoprotein in the interaction of digoxin and rifampin. J Clin Invest. 1999; 104:147–153. [PubMed: 10411543]
39. Schwarz UI, Hanso H, Oertel R, et al. Induction of intestinal P-glycoprotein by St John's wort reduces the oral bioavailability of talinolol. Clin Pharmacol Ther. 2007; 81:669–678. [PubMed: 17392718]
40. Prins ND, Scheltens P. Treating Alzheimer's disease with monoclonal antibodies: current status and outlook for the future. Alzheimers Res Ther. 2013; 5:56. [PubMed: 24216217]

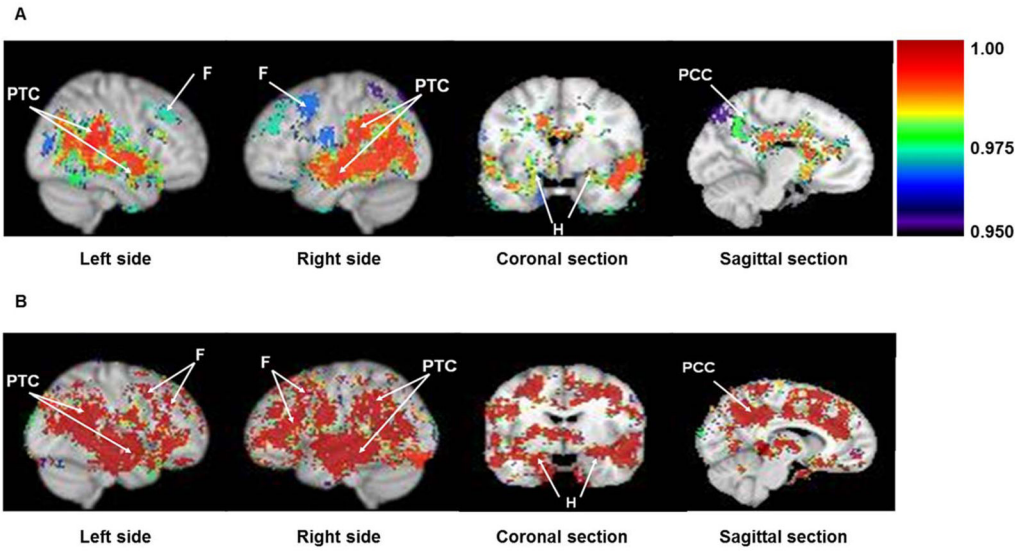

Figure 1.

Difference in regional cerebral blood flow (rCBFc) (A) and relative verapamil extraction ratio (ERc) (B) in AD vs. Controls. Grouped statistical brain parametric image comparisons (AD vs. controls) in sagittal, coronal and mid-sagittal planes show significant decrease in rCBFc (A) or P-gp activity (higher ERc) (B) in parietotemporal cortex (PTC), frontal lobe (F), hippocampus (H) and posterior cingulate cortex (PCC) in AD patients. Colored statistical parametric grouped brain images are shown as a thresholded overlay (threshold set to 0.95 which equals p=0.05) on top of the standard Montreal Neurological Institute (MNI) brain made from 152 coregistered brains placed into standardized MNI coordinate space. Color index is shown as probability statistical values (1-p) with higher significance represented as a higher value (i.e. lower CBFc in A and greater ERc or lower P-gp activity in B).

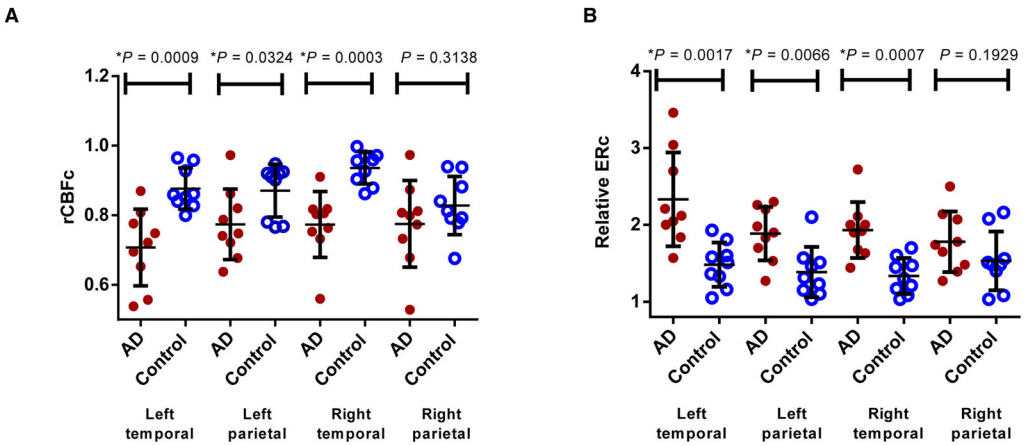

Figure 2.

Regions of interest analysis (ROI) in AD vs Control. ROI analysis of the parametric maps shows significantly lower regional cerebral blood flow (rCBF) (A) and P-gp activity (higher relative verapamil extraction ratios (ERc)) (B) in the temporal and left parietal cortices of AD patients vs. controls. Data are shown as mean±SD.

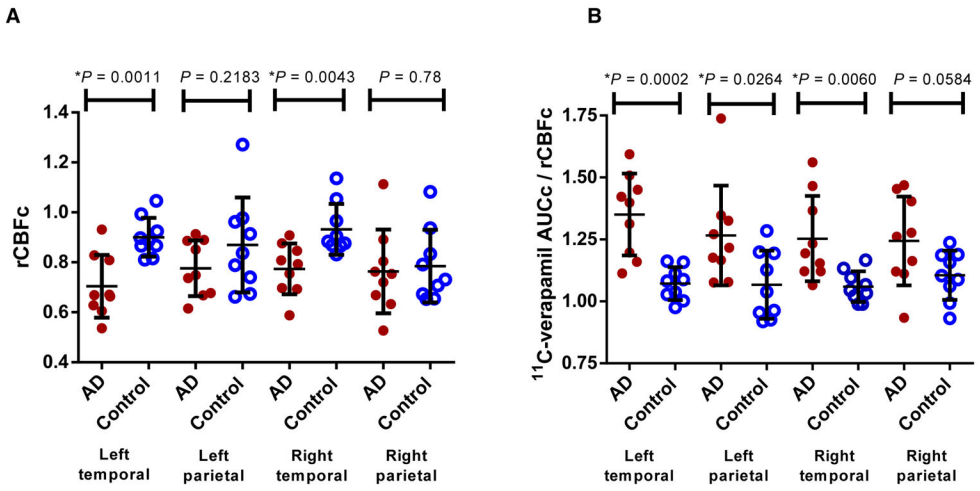

Figure 3.

Semiparametric analysis in AD vs Control. Semi-parametric region of interest analysis shows significant decrease in regional cerebral blood flow (rCBFc) in the temporal cortex (A) or P-gp activity (higher [^{11}C]-verapamil AUCc/rCBFc) (B) in the parietotemporal cortex of AD patients vs. controls. Data are shown as mean±SD.

Table 1

Profile of subjects enrolled in the study.

Profile	AD Patients n=9	Healthy Controls n=9
Age	73.2±1.9†	72.9±2.0
Weight (kg)	76.7±14.6	70.4±12.8
Education (years)	17.3±1.8	18.4±1.5
Gender (males/females)	7/2	4/5
Stage (CDR mean, range)	1.0 (1,1)	0.0 (0,0)
MMSE	24.3±1.6*	29.7±0.7
Mini-Cog™	1.4±1.2*	4.9±(0.5)

*p<0.0001, by unpaired two-tailed *t*-test.

†Values represent mean ± SD.MMSE= Mini-Mental State Examination, scores range from 0–30; CDR = Clinical Dementia Rating, 0 = normal cognition and 1 = mild dementia; Mini-Cog™ scores range from 0–5.